AMBIENT AEROSOL SAMPLING INLET FOR FLOW RATES OF

100 AND 400 L/MIN

A Thesis

by

MICHAEL MATTHEW BAEHL

Submitted to the Office of Graduate Studies of
Texas A&M University
in partial fulfillment of the requirements for the degree of

MASTER OF SCIENCE

December 2007

Major Subject: Mechanical Engineering

AMBIENT AEROSOL SAMPLING INLET FOR FLOW RATES OF

100 AND 400 L/MIN

A Thesis

by

MICHAEL MATTHEW BAEHL

Submitted to the Office of Graduate Studies of
Texas A&M University
in partial fulfillment of the requirements for the degree of

MASTER OF SCIENCE

Approved by:

Chair of Committee,   Andrew R. McFarland
Committee Members, Yassin A. Hassan
                                 Bryan W. Shaw
Head of Department, Dennis L. O'Neal

December 2007

Major Subject: Mechanical Engineering

ABSTRACT

Ambient Aerosol Sampling Inlet for Flow Rates of

100 And 400 L/min.   (December 2007)

Michael Matthew Baehl, B.S., University of Illinois, Urbana-Champaign

Chair of Advisory Committee: Dr. Andrew R. McFarland

New bioaerosol sampling inlets were designed and tested that have nominal
exhaust flow rates of 100 L/min to 400 L/min, and which have internal fractionators and
screens to scalp large, unwanted particles and debris from the transmitted size
distribution. These units consist of the same aspiration section, which is a 100 L/min
Bell Shaped Inlet (BSI-100), and different pre-separators. The pre-separators are called
the IRI-100 (Inline Real Impactor) with an exhaust flow rate of 100 L/min, the IRI-400
(exhaust flow rate of 400 L/min), the IVI-300 (Inline Virtual Impactor for a flow rate of
300 L/min) and the IVI-400. These units were tested in a wind tunnel at speeds of 2, 8,
and 24 km/hr with particle sizes between 3 and 20 μm AD (aerodynamic diameter). The
units show wind independent characteristics over the range of wind speeds tested. The
aspiration section of the BSI-100 has greater than 85% penetration for particle sizes ≤ 10
μm AD. The IRI-100, IRI-400, IVI-300 and IVI-400, when combined with the BSI-100
all provide cutpoints of 11 ± 0.5 μm AD.

ACKNOWLEDGEMENTS

TABLE OF CONTENTS

INTRODUCTION

Background

Hazardous bioaerosols in the ambient environment are a concern to society and early detection is needed to identify those that are potential threats. To achieve early detection, an effective inlet system is needed to provide detection/identification apparatus with an appropriate sample. In general, the particle size range that is currently required to be delivered by the inlet is taken to be the PM-10 fraction (particles with sizes ≤ 10 µm aerodynamic diameter, AD), which are sizes that can penetrate the human respiratory system to thoracic region (National Research Council, 2004). Stripping larger particles from the size distribution is accomplished with a pre-separator in the inlet, which fractionates the particles at a prescribed cutpoint. To fractionate ambient aerosol, various pre-separators have been utilized. There have been designs that use a cup impactor, where an oiled-surface is used to keep the particles from bouncing back into the main stream (Marple and Willeke 1976). This particle impactor cup has been used in other designs (Kim et al. 2002) to strip particles with sizes > 2.5 µm AD and allow transmission of the PM-2.5 aerosol to a filter collector. Another inlet was developed using a modified Andersen impactor and an all weather sampler inlet (McFarland 1977). The previous Andersen impactor collected 50% of particles larger than 7 and the new design was to collect particles as large as 14 µm. Another purpose of this study was to have the penetration through the inlet unaffected by wind speed in the range of 5.5-16.5 km/hr.

_____

This thesis follows the style and format of *Aerosol Science and Technology*.

Under the present study, two new PM-10-type inlets have been developed that employ a real impactor and a virtual impactor as pre-separators. The devices have been coupled with an existing inlet aspiration section (Nene, 2005), Figure 1, to accommodate bioaerosol sampling over the range of wind speeds of 2 to 24 km/h, with constant performance. The new pre-separators were designed to extend the size range slightly to a cutpoint (particle size for which the aerosol transmission is 50%) of about 12 μm AD as compared with the 10 μm AD cutpoint of a PM-10 inlet. This will allow more 10 μm AD aerosol particles to be delivered to a concentrator or collector, yet will still preclude the transmission of large pollen particles and other large background aerosol particles.

Motivations and Objectives

The goal of this study was to design and optimize bioaerosol sampling inlets for flow rates of 100 to 400 L/min. These inlets utilize the same aspiration section, which also serves as a common housing for the pre-separators, Figure 1; however, internal components of the fractionator need to be changed to accommodate the different flow rates or the different pre-separator approach. The tasks that were undertaken in this in this study are:

- Design and fabricate an inlet and fractionators for operation at nominal exhaust flow rates 100 and 400 L/min. The desired cutpoints are about 11 μm AD.
- Evaluate the designs for particle sizes ranging from 3 to 19 μm at wind speeds of 2, 8 and 24 km/hr.
- Assess aerosol particle losses on 8 and 16 mesh insect screens.
- Test the retention of large-sized dust particles in the pre-separators.

DESIGN

BSI/IRI Design

The aspiration section of a Bell-Shaped Inlet (see Figure 1) for a flow rate of 100 L/min (BSI-100) was previously designed and tested by Nene (2005). In the present study, the BSI-100 inlet was employed for sampling at nominal system exhaust flow rates from 100 to 400 L/min, and was fitted with pre-separators for the different flow rates. Figure 2 is a schematic diagram of the inlet, showing the aspiration section, an In-Line Real Impactor (IRI) and a bug screen. Labeled as 1 on the schematic diagram is the aspiration section, and labeled as 4 is the impaction plate where an oiled media collection surface is placed. The function of the oiled media surface is to retain particles that impact on the surface, i.e., keep them from either rebounding from the collection surface or prevent deposits of particles from being re-entrained . The combination of these two phenomena is called "solid particle carryover." The cone fractionator is labeled 5 on the schematic and the mesh screen is labeled 2. Figure 3 depicts a photograph of all the major components for the BSI-100 and both the IRI-100 and IRI-400.

The cone-shaped fractionator operates on the principle of inertial impaction, where an accelerated stream of aerosol is directed against an impaction plate. Here, the aerosol is accelerated in the gap between the cone and the inner wall of the tube (labeled 3 in Figure 2). A larger diameter cone will produce a higher velocity and thereby a smaller cutpoint for the impactor. The effect of cone size on aerosol penetration was tested using several different cones. Cone A is 88.9 mm (3.5-inches), Cone B is 92.25 mm (3.75-inches), Cone C is 105.41 mm (4.15-inches), and Cone D is 113.03 mm (4.45-inches) diameter. Two particle sizes were used in the tests and several volumetric flow

rates were employed to achieve the desired Stoke numbers, *Stk*, where the Stokes number is defined as:

$$Stk = \frac{\rho_p d_p^2 U_o C_c}{9 \eta W} \tag{1}$$

Here ρ_p is the density of the particle, d_p is the particle diameter, C_c is the Cunningham Correction factor, η is the viscosity of air, U_o is the air velocity in the gap between the base of the cone and the adjacent tube wall, and W is the gap between the cone base and the tube wall. For this design, the inner diameter of the tube is fixed at 103.175 mm (4.062 inches). As would be expected, changing of cone diameter and flow rate does have a major impact on the performance of the design. The reason for this is seen in equation 1, by changing W or U_o the Stokes number is changed giving a different particle size cutpoints to the system. From Figure 4, it can be noted the cutpoint Stokes number is approximately 0.53 for Cone D at 400 L/min.

For a classical inertial impactor, the ratio of the standoff distance, *S*, which is the distance between collection surface and the acceleration jet exit-plane characteristic dimension, *W*, can have a slight effect on the transmission (Hinds 1999). In Figure 2, *S* is labeled 6 and *W* is labeled 3. Tests were conducted with different values of *S/W*, which produced the results shown in Figure 5. The *S/W* ratios used in the inlets are a ratio of 3.74 for the 400 L/min setup 3.77 for the 100 L/min setup. It may be noted from Figure 5 that minor the value of *S/W* is not critical, so the data for *S/W* = 4, which are given in Figure 5, can be used to obtain the cutpoint Stokes number. In turn that cutpoint Stokes number can be used to find the correct cone sizes that give the desired cutpoint particle size. The cone size calculated for a cutpoint of 12 μm AD at 400 L/min is 88.47 mm

(3.483-inches) and the cone size for the same cutpoint at 100 L/min is 97.54 mm (3.84-inches). The cones that were tested are 88.9 mm (3.5-inches) for the 400 L/min and 97.79 mm (3.85-inches) for the 100 L/min.

BSI/IVI Design

The In-Line Virtual Impactor design (Seshadri 2007), shown in Figure 6, is intended to serve the same function as the IRI, in that it is a pre-separator with a cutpoint of about 11.5 µm AD. Both the IVI and IRI utilize a cone to accelerate and separate the particles, but instead of impacting the larger particles in an oiled media, the IVI takes the large particles out of the system through the minor flow channel. Figure 7 shows a schematic of the IVI design. Design of the critical zone key for the device to get the required particle size cutpoint. Primarily the cutpoint is a function of the gap width and the velocity in the gap between the cone base and the inner wall of the tube, however, the *H/W* ratio can be somewhat altered by varying the height of the alignment spacers to create a different particle size cutpoint. The larger particles are transported out of the critical zone by minor flow of 10% of the total inlet flow. The IVI-300 runs at an inlet flow of 333 L/min with 300 L/min flow exhausted as the major flow and 33 L/min exhausted as the minor flow. The IVI-400 has an inlet flow of 444 L/min with 400 L/min exhausted as the major flow and 44 L/min exhausted as the minor flow. The other difference between the IVIs is that the IVI-400 has a larger spacing, *S* than the IVI-300. The IVI-400 was tested the same way as the IRI pre-separators in the wind tunnel. Figure 8 shows the setup of the IVI in the wind tunnel.

EXPERIMENTAL PROTOCOL

General

The inlet and fractionator were tested for aerosol transmission with a 0.86 m (34-inches) wind tunnel using monodispersed fluorescently-tagged oleic acid droplets generated using a vibrating orifice aerosol generator (VOAG, Model 3050, TSI, Inc., Shoreview, MN). Figures 9 and 10 shows the overall test setup with the components necessary to run these experiments. Shown in Figure 9 is an air blender which creates uniformity of the concentration of the particles across the cross section of the wind tunnel. Downstream from that is a flow straightener that eliminates large-scale turbulence and flow swirl. A TSI VelociCalc thermal anemometer (TSI Inc., St. Paul, MN) is used to measure the wind speed in the wind tunnel, where three different speeds were employed; namely 2, 8, and 24 km/hr.

The aerosol particles used in these tests were generated from ethanol dilutions of a master solution containing 90% ethanol, 9% oleic acid and 1% sodium fluorescein by volume. The ethanol in the mixture evaporates leaving the oleic acid and sodium fluorescein to be sampled in the experiment. The dilution approach allowed particles to be generated over the size range from 3 to 20 μm in the VOAG. Table 1 shows the ratios of dilution needed for the corresponding particle size. The actual particle size of the residual droplets is determined by impacting a sample of the droplets on a glass slide that has been treated with an oil-phobic agent (a 0.2% solution of Nyebar K, William F. Nye, Inc., New Bedford, Mass.). Particle sizes on the slides are measured with a calibrated microscope and the true sizes of the droplets in the aerosol state are determined by taking into account the flattening of the droplets on the slide through use of a coefficient similar

to that of Olan-Figuroa et al. (1982), but with a value of 1.29, which is appropriate for the Nyebar K. An Aerodynamic Particle Sizer (APS, Model 3321, TSI Inc., St. Paul, MN) is used to monitor the aerosol during a test for assurance that neither the size nor the concentration changes.

Wind Tunnel Testing with Monodispersed Aerosols

During wind tunnel tests, two isokinetic nozzles and the test inlet are mounted in the free jet at the end of the wind tunnel, where the isokinetic nozzles are used to provide the reference concentration of the aerosols. Aerosol transmitted through the isokinetic nozzles and the test inlet is collected on glass fiber filters (Type A/E, Pall Corporation, East Hills, NY). Air flow rates through the isokinetic nozzles and the inlet are determined through use of rotameters (Dwyer Instruments, Michigan City, IN) and Magnehelic differential pressure gages (Dwyer Instruments, Michigan City, IN). Wall losses can occur on the isokinetic nozzles, and because the reference samples are based on all particles that cross the inlet plane of an isokinetic nozzle, the wall losses must be recovered. This is done by cleaning the inner surface of an isokinetic nozzle with an isopropyl solution and recovering the wash solution. The mass of aerosol calculated from this wall loss is then added to the mass based on the filter sample.

The aerosol collection filters are analyzed by first soaking them in 60 mL of isopropyl alcohol and water solutions (2/3 alcohol and 1/3 water, v/v) for at least four hours to elute the fluorescent tracer. A 4 mL aliquot of this solution is placed in a test tube and 1 drop of 1 molar NaOH is added to stabilize the fluorescence (Kesevan et al. 2001). The concentration of fluorescein is measured with a fluorometer (Turner

Quantech Model 450 Digital Filter Fluorometer, Barnstead International, Dubuque, IA)
that is fitted with NB490 and SC515 filters optical filters. The wall loss samples from the
isokinetic nozzles are also analyzed fluorimetically, with 4 mL aliquots of solution plus
one drop of 1 molar NaOH being tested.   The relative concentration of aerosol sampled
by the inlet based on the particular sample being evaluated is:

$$C = \frac{R \cdot V}{Q \cdot t} \qquad (2)$$

where C is the calculated relative concentration of particulate matter in the aerosol state,
R is the fluorometer reading, V is the solution volume, Q is the corrected air flow rate,
and t is the time for particle collection. The aerosol transmission is calculated from:

$$T = \frac{C_{inlet}}{C_{iso} + C_{iso,w}} \qquad (3)$$

where C_{inlet} is the concentration based on the after-filter on the test inlet; C_{iso} is the
average concentration based on the after-filters of the isokinetic nozzles; and, $C_{iso,w}$ is the
average concentration based on the wall losses in the isokinetic nozzles.

The air flow rates measured by the rotameters need to be to be corrected for
pressure (the readings stamped on a rotameter face are for standard pressure and
temperature). This is accomplished by:

$$Q_2 = Q_1 \times \sqrt{\frac{P_2}{P_1}} \qquad (4)$$

where Q_2 is the corrected air flow rate, Q_1 is the flow rate measured, P_2 is the standard
atmospheric pressure minus the measured pressure, and P_1 is the standard atmospheric
pressure (101.3 kPa). Here, it is assumed the temperature correction is negligible.

Each test condition is replicated at least three times and the transmission is the average of those three tests. All tests are also operated for a time period that is sufficient for the signal from the collected fluorescein to be at least one order of magnitude larger than the background. Test times vary depending on particle size and wind speed.

Static Testing with Heterogeneous Dusts

Static loading tests with test dusts were conducted to examine the range of dust loadings over which the pre-separators would function acceptably. Figure 11 shows the complete test setup and testing area. The BSI-100 is not used in these tests, only the pre-separator section of the inlets. Both Fine (ISO 12103-1, A2 Fine Test Dust) and Coarse (ISO 12103-1, A4 Coarse Test Dust) Arizona Road Dust, ARD, were used in testing the pre-separators.

For the IRI, three types of impaction surfaces were tested, namely:

1. Impaction Plate – smooth aluminum shim.

2. Plate with Grease – shim with Dow Corning high vacuum grease.

3. Oil Surface - Dow Corning 704 Diffusion Pump Fluid as impaction surface.

The different impaction surfaces can be seen in Figure 12. These different impaction surfaces were tested with both the IRI-100 and IRI-400 setups operated at 100 L/min and 400 L/min, respectively. Besides the flow rate for each setup, the difference is the cone size which is 88.9 mm (3.5-inches) in diameter for the 400 L/min flow rate and 97.79 mm (3.85-inches) in diameter for the 100 L/min flow rate. In these tests a shot of the dust is aerosolized with a glass nebulizer (Product number: 14606, TED PELLA, Inc. Redding, CA). Each shot was comprised of a measured amount of dust, which was between 0.1

and 0.15 g. The dust transmitted through the IRI is then collected on pre-weighted 102 mm diameter glass fiber filters, which are re-weighted at the completion of a test. Transmission is then calculated from the final weight of the filter divided by the total amount of dust injected into the system.

QUALITY ASSURANCE

Aerosol Quality

The monodispersed fluorescently-tagged oleic acid droplets used in this study were generated with a vibrating orifice aerosol generator (VOAG, Model 3050, TSI, Inc., Shoreview, MN). These aerosols need to be monodispersed in size and have uniformity of concentration across the test region of the wind tunnel. An Aerodynamic Particle Sizer (APS, Model 3321, TSI Inc., St. Paul, MN) is used for assurance that the aerosols are monodispersed. The size of the particle is also very important to the test. To measure the size the particles are impacted on a glass slide treated with 0.2% Nyebar K, and droplet diameters are measured with an optical microscope using a calibrated stage micrometer. Particles samples are collected before and after each test to be sure the size remains constant. Under the microscope, particles are measured in the peripheral of the impaction zone to help reduce the chance of measuring a doublet. At least 5 particles are measured before equating the size of the particle. The calculation for the aerodynamic diameter, D_a, is:

$$D_a = D_p \times (\frac{\rho_p}{\rho_0})^{\frac{1}{2}} \tag{5}$$

where D_p is the physical diameter of the droplets; and, ρ_0 is the density of water at 4ºC (1000 kg/m³). The density of the droplets, ρ_p is determined by measuring the density of the mixture which is about 90% oleic acid and 10% sodium fluorescein (volume to mass). The density of the droplets for this experiment is 934 kg/m³. The physical diameter of the droplets is the value obtained by multiplying the size measured under the microscope by the flattening factor of 1.29.

Two isokinetic nozzles are used as references to average any non-uniformity of concentration of the particles across the test cross-section of the wind tunnel. Figure 13 shows the location of the isokinetic nozzles relative to the wind tunnel and inlet. Figure 14 shows a photograph of the inlet and isokinetic nozzles.

Fluorometer Analysis Quality

To measure the concentration collected on the filters, a fluorometer Kesavan et al. (2001) studied and found that the optimum excitation and emission wavelengths for fluorescein are 492 nm and 516 nm, respectively. Therefore NB490 and SC515 filters are used in the fluorometer. The fluorescence intensity from a fluorescein solution is also pH dependent, but for pH values above 8, the intensity is both maximized and constant (Kesavan et al., 2001). To fulfill this requirement one drop of 1N NaOH is added to each 4mL aliquot.

ERROR ANALYSIS

In all experimental tests there is a degree of uncertainty. Uncertainty takes into account two parts: systematic errors and precision errors. Systematic errors which could occur in the wind tunnel tests, could for example arise from contamination of the samples. The air sampling filter that are used to find the transmission of particles through the inlets could be contaminated with extra fluorescein from the containers in which they are soaked, or by the implements that are used to handle them. Therefore it is imperative to take care of such things and wash the containers well before using them. These systematic errors can be minimized if proper care is taken.

Precision errors are normally associated with the random variability of measurement devices. Precision errors can be quantified by using the Kline and McClintock (Nene 2005) method. The two equations whose uncertainty needs to be examined are those for the Stokes number and the transmission. The equation used for the transmission is Equation 2 and for the Stokes number is Equation 1. Uncertainty is defined by Kline and McClintock by:

$$w_R = \sqrt{\sum_{i=1}^{n}\left(\frac{\partial R}{\partial x_i}w_i\right)^2} \tag{6}$$

where w_R is the uncertainty in the result R, n is the number of independent variables with an associated uncertainty in the parameter R, x_i is the independent variable with an associated uncertainty, and w_i is the uncertainty in the variable x_i.

The transmission and the Stokes number can be shown in their measured quantities:

$$T_{calculated} = \left[\frac{R_{exp}}{R_{ref}}\right] \cdot \left[\frac{V_{exp}}{V_{ref}}\right] \cdot \left[\frac{Q_{ref}}{Q_{exp}}\right] \cdot \left[\frac{t_{ref}}{t_{exp}}\right] \tag{7}$$

$$Stk_{calculated} = \frac{\left(1 + \frac{2.34 \cdot \lambda}{d_p}\right) \cdot \rho_p \cdot D_p^{\,2} \cdot U_0}{9 \cdot \mu \cdot d_j} \tag{8}$$

where T is the aerosol transmission, R is the fluorometer reading in arbitrary units, V is the solution volume used to soak filters, Q is the corrected air flow rate, and t is the time for particle collection. For Equation 8, λ is the mean free path of air, D_p is the particle diameter, ρ_p is the density of the particle, U is the undisturbed air velocity, μ is the viscosity of air, and d_j is the characteristic dimension, taken to be the gap between the cone base and the inner wall of the cylinder.

To find the uncertainty of the transmission of the inlet measurable quantities R, V, and Q, are taken into account. The time duration and the scale of the fluorometer can be ignored. The uncertainty in the transmission of the inlet is shown as:

$$\frac{w_T}{T} = \sqrt{\sum \left(\frac{a_i w_{x_i}}{x_i}\right)^2} \tag{9}$$

$$\frac{w_T}{T} = \sqrt{\left(\frac{w_{R_{exp}}}{R_{exp}}\right)^2 + \left(\frac{-w_{R_{ref}}}{R_{ref}}\right)^2 + \left(\frac{w_{V_{exp}}}{V_{exp}}\right)^2 + \left(\frac{-w_{V_{ref}}}{V_{ref}}\right)^2 + \left(\frac{-w_{Q_{exp}}}{Q_{exp}}\right)^2 + \left(\frac{w_{Q_{ref}}}{Q_{ref}}\right)^2} \tag{10}$$

where a_i is the exponent of each variable x_i. The uncertainties for R, V, and Q are estimated to be 5%, 1.25%, and 5% respectively, which gives the total uncertainty for the transmission of the inlet to be 10.2%.

The uncertainty of the Stokes number is shown as:

$$w_{Stk} = \sqrt{\sum \left(\frac{\partial Stk}{\partial x_i} w_{x_i} \right)^2} \tag{11}$$

To find the uncertainty in the Stokes number D_p, U, and d_j are taken into account. The mean free path of air λ and the viscosity of air μ have errors that are assumed to be negligible.

The Stokes number can be rewritten as,

$$Stk = \frac{(D_p^2 + 2.34 \cdot \lambda \cdot D_p) \cdot \rho_p \cdot U_0}{9 \cdot \mu \cdot d_j} \tag{12}$$

after partially differentiation of the desired variables:

$$\frac{\partial Stk}{\partial D_p} = \left(\frac{2 \cdot D_p + 2.34 \cdot \lambda}{D_p + 2.34 \cdot \lambda} \right) \cdot \frac{Stk}{D_p} \tag{13}$$

$$\frac{\partial Stk}{\partial U} = \frac{Stk}{U} \tag{14}$$

$$\frac{\partial Stk}{\partial d_j} = -\frac{Stk}{d_j} \tag{15}$$

The uncertainty equation for Stokes number is thus:

$$\frac{w_{Stk}}{Stk} = \sqrt{\left[\left(\frac{2 \cdot D_p + 2.34 \cdot \lambda}{D_p + 2.34 \cdot \lambda} \right) \cdot \left(\frac{w_{D_p}}{D_p} \right) \right]^2 + \left(\frac{w_U}{U} \right)^2 + \left(\frac{w_{d_j}}{d_j} \right)^2} \tag{16}$$

The uncertainty in U and d_j are estimated to be 3% and 0.2%, respectively. The uncertainty for measuring particle sizes of 5, 10, 15 and 20 μm AD are estimated to be 4%, 2%, 1% and 1%, respectively. The uncertainty for Stokes number is then 8.4%, 5%, 4% and 3.6% for the particle sizes of 5, 10, 15 and 20 μm AD, respectively.

RESULTS AND DISCUSSION

BSI-100 Inlet

Initially, tests were conducted to determine aerosol penetration through the aspiration section alone, to verify the results of Nene (2005). Results from these tests, and the comparative data of Nene are shown in Figures 15 and 16. Figure 15 shows the penetration as a function of wind speed and particle size for the 100 L/min flow rate and Figure 16 shows the results for 400 L/min. For both flow rates, there is little dependency on wind speed at sizes smaller than about 12 μm AD). The results of the present study at 100 L/min compare will with those of Nene. The comparative results are within 5% for particles sizes ≤ 10 μm AD for all wind speeds. The data at 2 and 8 km/hr are still close even at 15.5 μm AD, although the data for 24 km/differ by about 17% at the largest particle size. This difference is accentuated by the steep slope of the curves for the larger particle sizes.

A screen is necessary in the inlet to keep bugs and very large debris (e.g., cottonwood seeds) from being transmitted through the system. Either an 8 or 16 mesh wire screen is to be installed directly above the cone fractionator. Figure 17 shows the results of the tests done with wire screens placed in a test housing. The aspiration section of the inlet was removed for these tests, nor were pre-separators included in the test fixtures. These tests were conducted at both 100 and 400 L/min flow rates. At 100 L/min there is a negligible loss of small particles on either the 8 or 16 mesh screen. At 400 L/min there is approximately a 7% loss of a particle size of 10 μm and a 10% loss of particle size of 14 μm on either the 8 or 16 mesh screen. This data can be seen in Tables

3-10. With regards to the results of these tests, either the 8 or 16 screen mesh could be used at either flow rate with losses of less than 10% for particles as large as 14 µm AD.

BSI-100 IRI

Tests were conducted to find the correct cone diameter and height for the 100 L/min flow rate setup in order to achieve a cutpoint of about 12 µm AD. Table 2 lists the critical dimensions for both the IRI-100 and IRI-400. A 97.79 mm (3.85-inches) diameter cone along with a standoff distance of 10.16 mm (0.4-inches) from the impaction surface (S/W = 3.77) is gives a cutpoint of 11.5 µm AD.   Figure 18 displays the transmission as a function of particle size from wind tunnel tests. There is close to 100% transmission for particles ≤ 3 µm AD and approximately 10% or less transmission for particles with sizes ≥ 15 µm AD. Further testing was done on the 88.9 mm (3.5-inches) cone at a height of 26.72 mm (1.052-inches) for the 400 L/min flow rates. Figure 19 shows the transmission with respect to the different particle sizes tested. It follows the same trend as the BSI-100 IRI-100. These graphs give an expected trend where the cutpoint is approximately 11.5 µm AD.

Figure 20 shows the transmission of aerosol particles through the BSI-100/IRI-400 with respect to the different wind speeds tested. This graph gives a good sense of the independence the device has on wind speed. At 2, 8 or 24 km/hr the transmission is within 7%. These graphs show the cutpoint is approximately 11.5 µm AD.

Solid Particle Carryover

Wind tunnel tests provide characteristic fractional efficiency curves for liquid particles, but it is important to also characterize the performance of the fractionator with solid particles. Focusing on the three main ways of collecting large solid particles (bare impaction plate, plate with grease, and oiled surface) tests were conducted with Arizona Road Dust. For the IRI-100, the ARD Fine and ARD Coarse results are shown in Figures 21 and 22, respectively. The corresponding results for the IRI-400 are shown in Figures 23 and 24. Figures 25-27 show photographs of solid particle collection on the bare impaction plate, the plate with a grease coating, and the oil surface, respectively. Comparing the width of the deposition band in Figure 25, the bare impaction surface, which is a smooth aluminum plate, with the bands for the grease coated surface (Figure 26) and the oiled surface (Figure 27) shows the bare impaction surface is carried away from the immediate zone under the acceleration jet. The grease coated surface shown in Figure 26 has a shim coated Dow Corning high vacuum grease, however, that also does not work well because after some of the dust is collected on the grease layer, additional dust will either rebound or be re-entrained from the dry dust surface. The oil coated surface shown in Figure 27, is Dow Corning 704 Diffusion Pump Fluid (Dow Corning, Midland, MI) soaked into a porous surface (Porex Filtration Group, Fairburn, GA). In this case, the collected particles are continually wet by the oil, and thereby better retained. For tests with both the IRI-100 and the IRI-400, and for both ARD Fine and ARD Coarse test dusts, the transmission is the least for the oiled collection surface, which implies that the solid particle carryover is least for that type of surface. The oil surface is thus best suited for use in the IRI. From calculations of the size volume distribution for

Fine ARD and the transmission curves of each inlet, it was found that out of 100 mg of Fine ARD that 43.3 mg will go through the IRI-100, 45.9 mg will go through the IRI-400, and 40.9 mg will go through the IVI-400 inlet. This corresponds very close to experimental results seen in Figures 21 and 23, which shows that about 40% of Fine ARD goes through both the IRI-100 and IRI-400.

BSI-100 IVI

Tests were also conducted with an IVI-100 configuration (flow rate of 100 L/min) with the help of Seshadri (2007). Figure 28 shows the results from those tests. There is a range of 85% to 95% transmission for the 3 μm AD particle size because approximately 10% of the flow is cut out of the system. The cutpoint for the IVI-100 is about 11 μm AD Figure 29 shows the characterization curve for the IVI-300 and the cutpoint is also about 11 μm AD. Figure 30 shows the characterization curve for the IVI-400. It can be determined from the graph that the cutpoint for the IVI-400 is 11.2 μm AD.

Figure 31 gives the comparison of particle size vs. transmission between the IVI-400 and the IRI-400. Both the IVI and IRI show the same trend overall and fall on the same line for 11 μm AD and higher. The IVI has less transmission for lower than 11 μm AD particle sizes and can only reach 90% transmission at the smallest particle size tested because of the 10% minor flow.

SUMMARY AND CONCLUSIONS

The purpose of this study is to design bioaerosol sampling inlets with fractionators that provide a cutpoint of about 11-12 μm AD. The inlets needed to be designed for air exhaust flow rates of 100 to 400 L/min. Another requirement needed for these inlets is that the performance is unaffected wind speed. Two designs have been presented in this thesis as working inlets and fractionators for sampling ambient bioaerosols.

While most tests were run with liquid particles, other testing on the IRIs was done with solid particles. Different impaction surfaces were tried to find the best results to minimize solid particle carryover. Results from those tests show that the oiled media works best for the application.

The IRI and IVI both utilize the same aspiration device, i.e., the BSI-100. The BSI-100 tested by itself shows that it is independent of wind speed for particle sizes ≤ 12 μm AD and only has minor losses of small particles. To keep very large debris out of the system such as bugs and cottonwood seed, a screen mesh was introduced to the system. The screen only offers a small loss of 10% to particle transmission at the high flow rate of 400 L/min and with a 14 μm AD particle size. As mentioned one of the biggest parts of the design was to be sure that the inlet worked independently of wind speed. Through testing these devices at 2, 8 and 24 km/hr it is shown that wind speed does not affect the inlet's performance. The IRI and IVI designs provide the needed cutpoint that is needed for these aerosols prior to the aerosol being concentrated or collected for analysis. Both designs have great advantages for aerosol collecting applications.

Overall, there are options are to utilize flow rates of 100, 300 or 400 L/min for aerosol sampling devices. While the IVI does not need an oiled surface to collect particles the IRI does not need extra design accommodations to draw the 10% minor flow that the IVI needs. The IRI can be used when there is low dust loading, there is not a significant number of large size particles, and occasional bounce of particles is not a problem. The IVI should be used in other cases. Depending on the application one can use the IRI-100, IVI-300, IVI-400 or the IRI-400 coupled with the BSI-100 housing.

REFERENCES

Hinds, W. C. (1999). *Aerosol Technology.* John Wiley & Sons, New York.

Kesavan, J., Doherty, R.W., Wise, D.G., and McFarland, A.R. (2001). Factors that Affect Fluorescein Analysis, Report ECBC-TR-208, Edgewood Chemical Biological Center, U.S. Army Soldier and Biological Chemical Command, Edgewood, MD.

Kim, H.T., Han, Y.T, Kim, Y.J., Lee, K.W., Chun, K.J. (2002). Design and Test of 2.5 μm Cutoff Size Inlet Based on a Particle Cup Impactor Configuration, *Aerosol Science and Technology* 36: 136-144.

Marple, V.A., Willeke, K. (1976). Impactor Design. *Atmospheric Environment* 10: 891-896.

McFarland, A.R., Wedding, J.B., Cermak, J.E. (1977). Wind Tunnel Evaluation of Modified Anderson Impactor and an All Weather Sampler Inlet. *Environmental Science and Technology* 11:387.

National Research Council. (2004). *Sensor Systems for Biological Agent Attacks: Protecting Buildings and Military Bases.* The National Academies Press, Washington, DC.

Nene, R. (2005). *Design of Bioaerosol Sampling Inlets.* M.S. Thesis, Texas A&M University, College Station, TX.

Olan-Figueroa, E., McFarland, A.R., and Ortiz, C.A. (1982). Flattening Coefficient for DOP and Oleic Acid Droplets Deposited on Treated Slides. *Am. Ind. Hyg. Assoc. J.* 43:395-399.

Seshadri, S. (2007). *The In-Line Virtual Impactor.* Ph.D Dissertation, Texas A&M University, College Station, TX.

Supplemental Sources Consulted

Biswas, P., and Flagan, R.C. (1988). The Particle Trap Impactor. *J. Aerosol Sci.* 19:113-121.

Chow, J. (1995). Measurement Methods to Determine Compliance with Ambient Air Quality Standards for Suspended Particles. *J. Air and Waste Manage. Assoc.* 45:320-382.

John, W., Winklmayr, W., Wang, H.C. (1991). Particle Deagglomeration and Re-entrainment in a PM-10 Sampler. *J. Aerosol Sci.* 14:165-176.

Jones, W., Morring, K., Morey, P., Sorenson, W. (1985). Evaluation of the Andersen Viable Impactor for Single Stage Sampling. *Am. Ind. Hyg. Assoc. J.* 46:294-298.

Kalatoor, S., Grinshpun, S.A., Willeke, K. (1995). Aerosol Sampling from Fluctuating Flows into Sharp-Edged Tubular Inlets. *J. Aerosol Sci.* 26:387-398.

Fatah, A. A., Barrett, J. A., Arcilesi, Jr., R. D., Ewing, K. J., Lattin, C. H., Moshier, T. F. (2001). An Introduction to Biological Agent Detection Equipment for Emergency First Responders. *National Institute of Justice Guide* 101-00.

Kim, H.T., Lee, K.W (2000). Sampling Inlet based on Particle Cup Impactor. *Journal of Aerosol Science* 31:S122-S123.

Liu, B.Y.H., Pui, D.Y.H. (1980). Aerosol Sampling Inlets and Inhalable Paricles. *Atmospheric Environment* 15:589-600.

McFarland, A.R., Ortiz, C.A., R.W. Bertch, Jr. (1984). A 10 μm Cutpoint Size Selective Inlet for Hi-Vol Samplers. *J. Air Pollut. Contr. Assoc.* 34:544-547.

McFarland, A.R., Wedding, J.B., Cermak, J.E. (1977). Large Particle Collection Characteristics of Ambient Aerosol Samplers. *Atmospheric Environment* 11:535-539.

Merrifield, T.M. (1988). Commercial U.S. PM10 Instruments. *J. Aerosol Sci.* 19: 1005-1008.

Okazaki, K. (1987). Transmission and Deposition Behavior of Aerosols in Sampling Inlets. *Aerosol Science and Technology.* 7:275-283.

Ranade, M.B., Woods, M.C., Chen, F-L. (1990). Wind Tunnel Evaluation of PM10 Samplers. *Aerosol Science and Technology.* 13:54-71.

Seo, Y. (2004). *Degree of Mixing Downstream of Rectangular Bends and Design of Inlets for Ambient Bio-Aerosol Sampling.* M.S. Thesis, Texas A&M University, College Station, TX.

Thompson, M.W., Donnelly, J., Grinshpun, S.A., Juozaitis, A., Willeke, K. (1994). Method and Test System for Evaluation of Bioaerosol Samplers. *J. Aerosol Sci.* 25:1579-1593.

Tolocka, M.P., Peters, T.M., Vanderpool, R.W., Chen, F., Wiener, R.W. (2001). On the Modification of the Low Flow-Rate PM_{10} Dichotomous Sampler Inlet. *Aerosol Science and Technology.* 34:407-415.

Wedding, J.B. (1982). Ambient Aerosol Sampling: History, Present Thinking and a Proposed Inlet for Inhalable Particulate Matter. *Environmental Science and Technology*. 16:154-161.

APPENDIX

Tables

Table 1: Approximate Particle Sizes Produced by VOAG solutions. Orifice size = 20 μm. Master solution is comprised of Oleic Acid, Sodium Flourscein and Ethanol.

Particle Size (um)	Oleic Acid/Fluorescein Master (mL)	Ethanol (mL)	Total Solution Vol (mL)
1	0.060	499.940	500
2	0.440	499.560	500
3	1.490	498.510	500
4	3.540	496.460	500
5	6.920	493.080	500
6	11.950	488.050	500
7	18.980	481.020	500
8	28.330	471.670	500
9	40.340	459.660	500
10	55.340	444.660	500
11	73.660	426.340	500
12	95.630	404.370	500
13	121.580	378.420	500
14	151.850	348.150	500
15	186.770	313.230	500
16	226.670	273.330	500
17	271.890	228.110	500
18	322.740	177.260	500
19	379.580	120.420	500
20	442.720	57.280	500

Table 2: Characteristic Dimensions for IRI-100 and IRI-400.

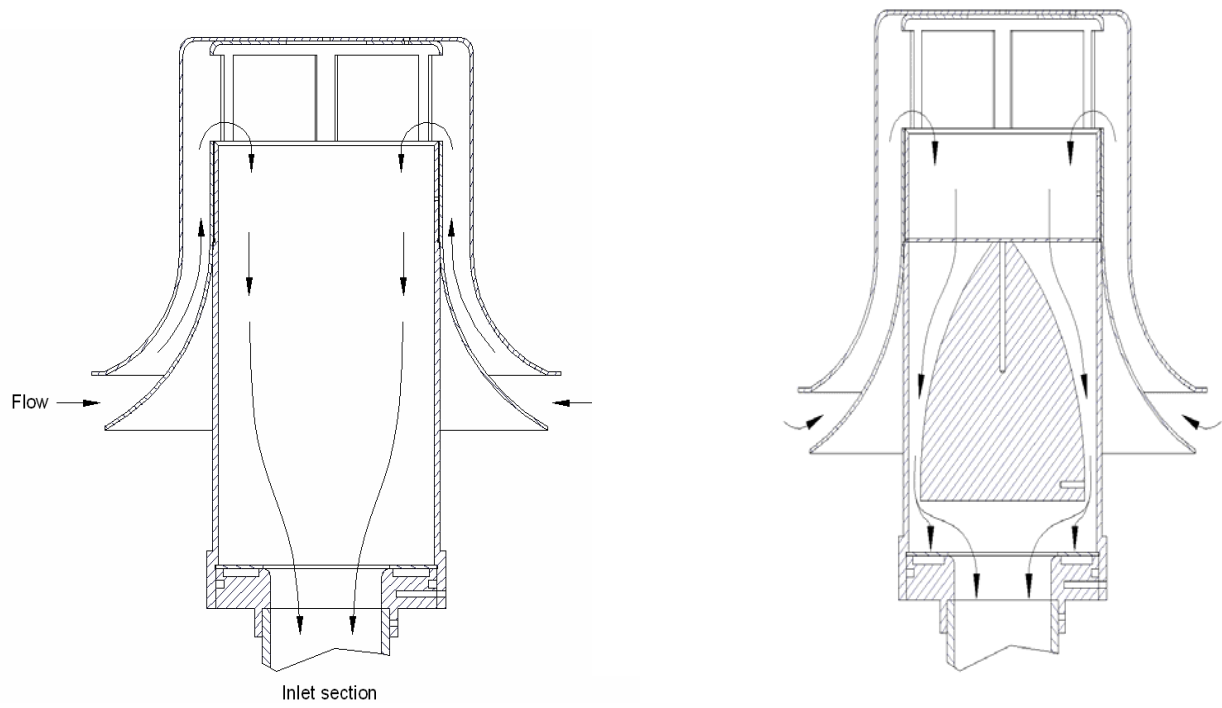|	IRI-100	IRI-400
Cone Diameter (mm.)	97.8	88.9
Gap Width (mm.)	2.69	7.14
Gap Height (mm.)	10.2	26.7
S/W	3.77	3.74

Figures

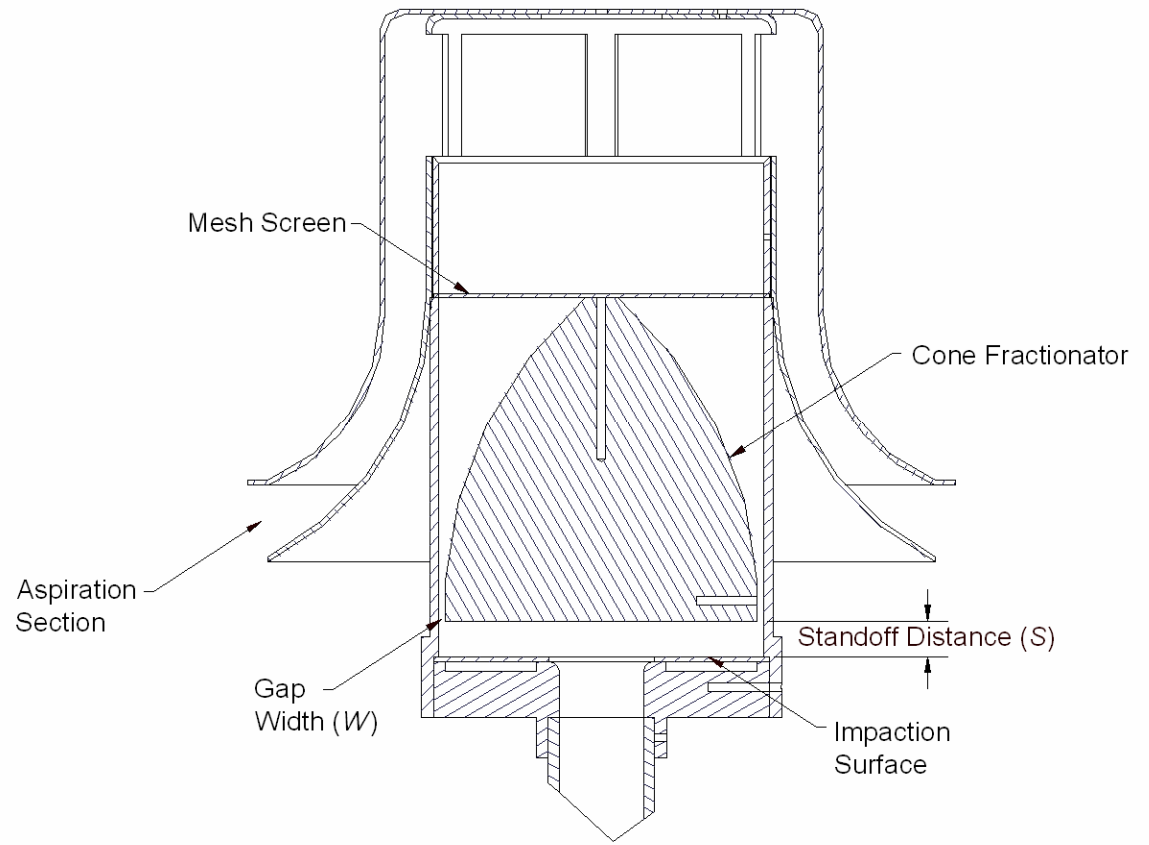**Figure 1:** Aspiration section (BSI-100) (left), with pre-separator (right).

Figure 2. Schematic of inlet, fractionator and screen (Not-to-Scale).
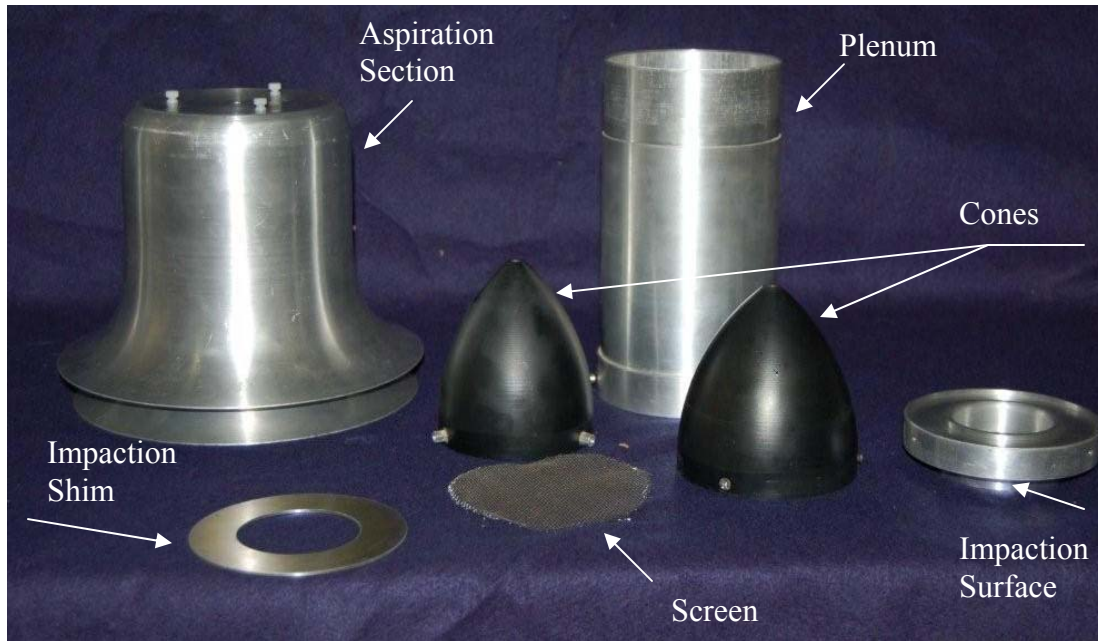
Figure 3: Photograph of exploded view of complete components of IRI-100 and IRI-400. Shown is the aspiration section, the mesh screen, the two different cones for the two flow rates, the impaction plate and surface, and the plenum.
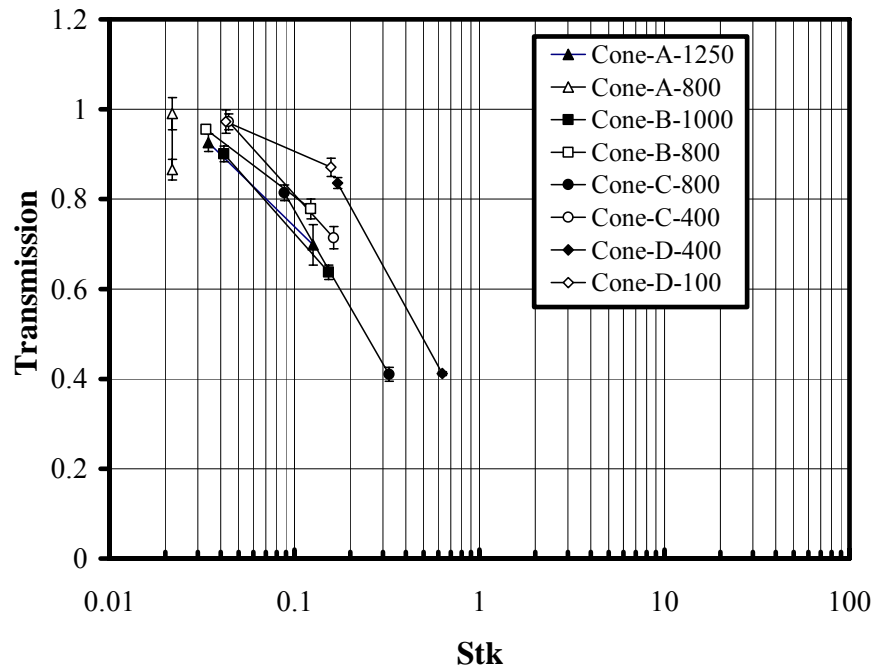
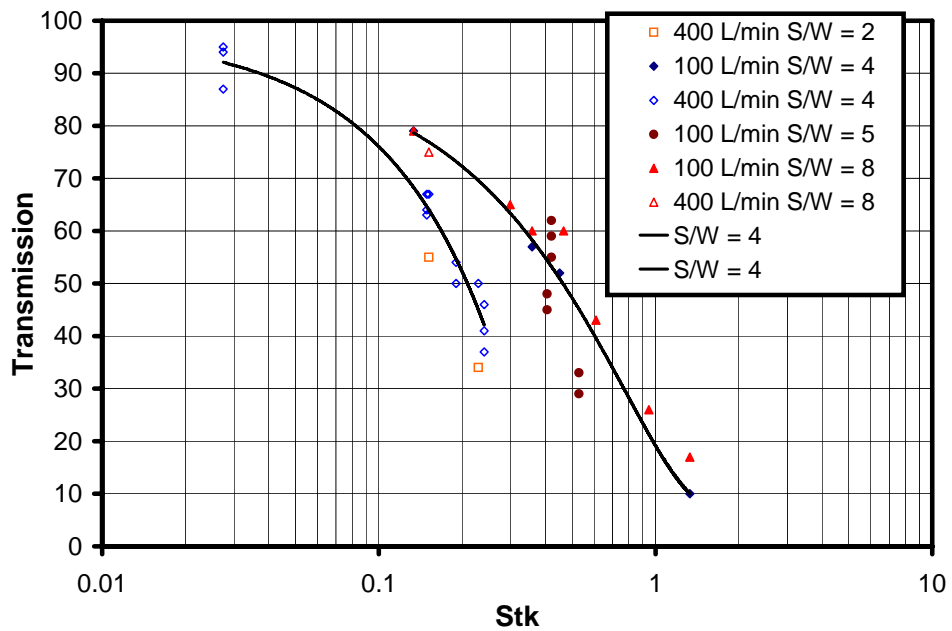**Figure 4.** Aerosol transmission for different size cones.

Figure 5. Transmission of aerosol particles through IRI units for different values of *S/W*. Curves are for *S/W* = 4.

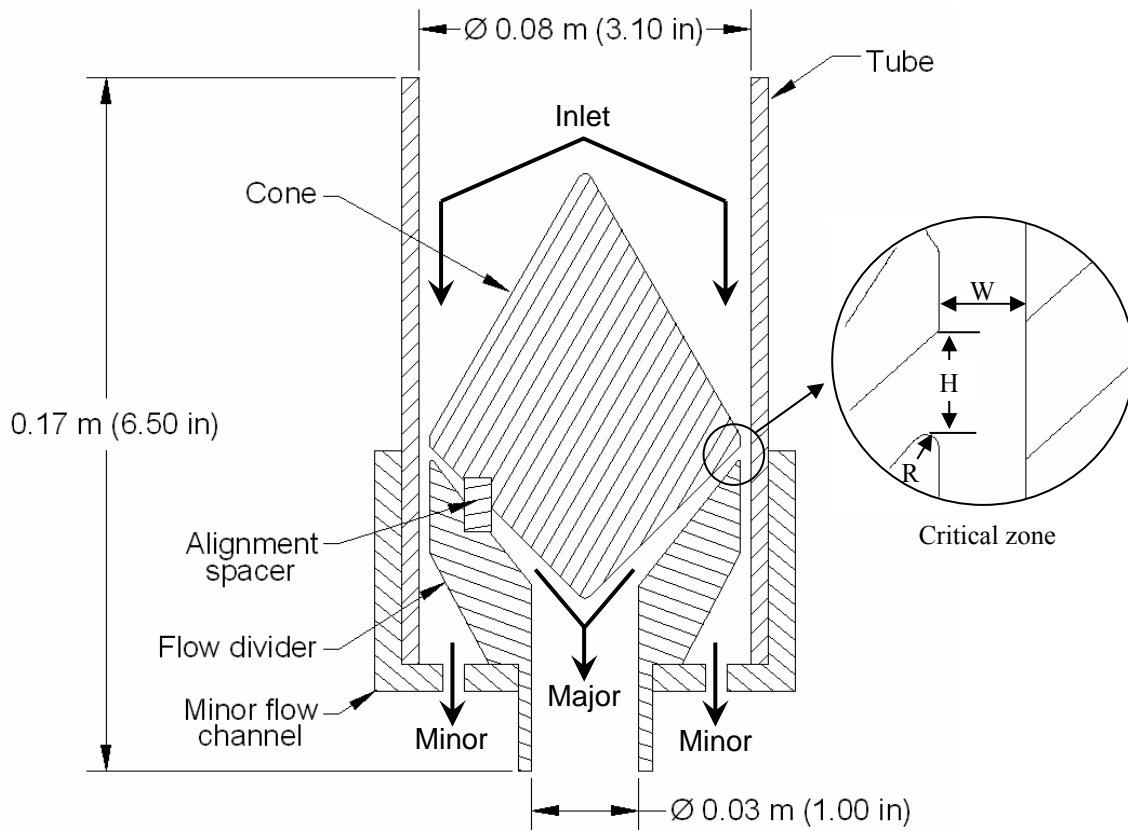**Figure 6:** Photograph of BSI-100/IVI-400 as used in experiments.

Figure 7: Schematic of IVI design.

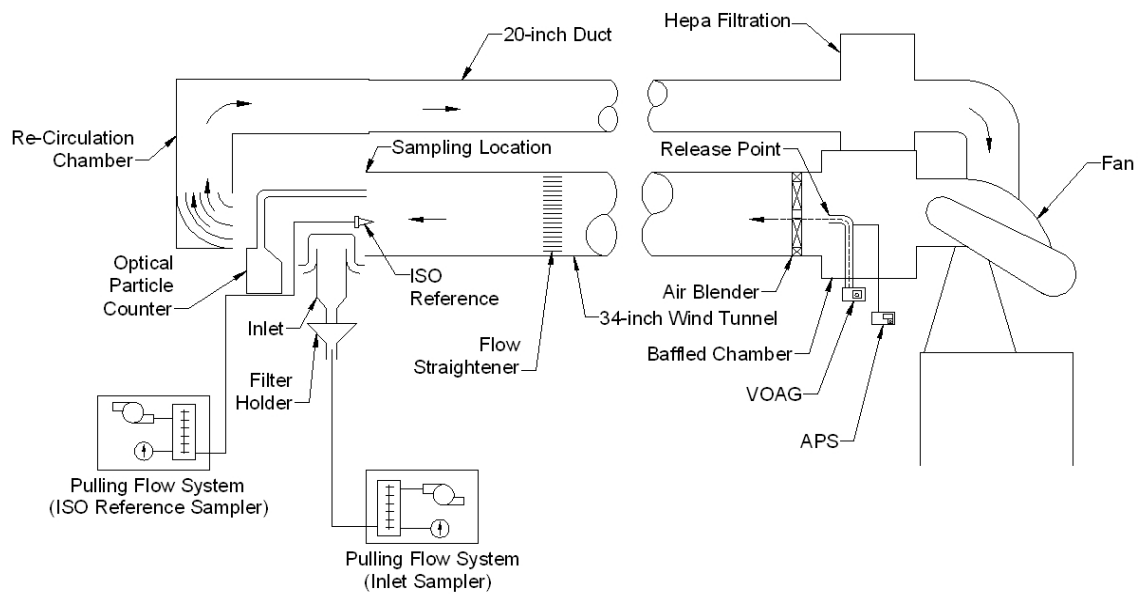**Figure 8:** Photograph of placement of BSI-100/IVI-400 in wind tunnel.

Figure 9: Schematic of wind tunnel and general test setup.

Figure 10: Photograph of wind tunnel and test setup.

Figure 11: Photograph of test setup of static load testing. Pictured here are the scales used to measure dust mass, a container of Fine ARD, and the IRI setup for this test.
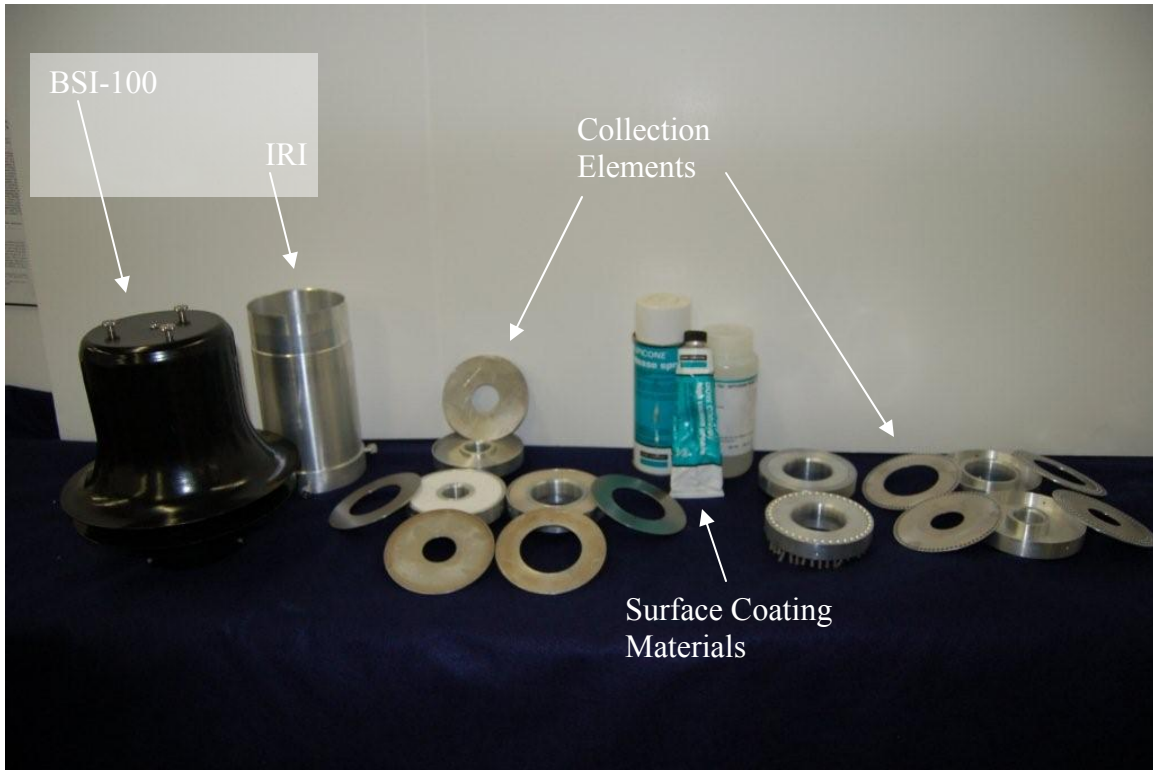
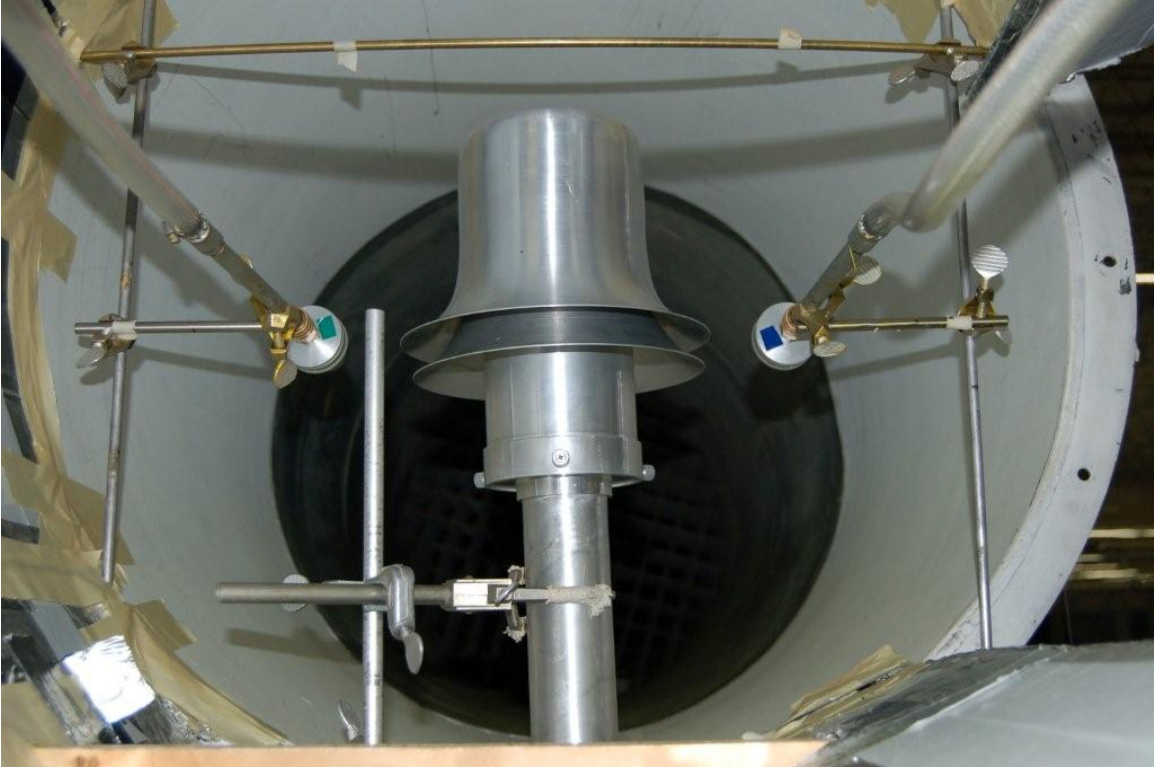**Figure 12:** Photograph of devices tested for impaction surface during static load testing.

Figure 13: Photograph of placement of BSI-100 and isokinetic nozzles at test section of wind tunnel.

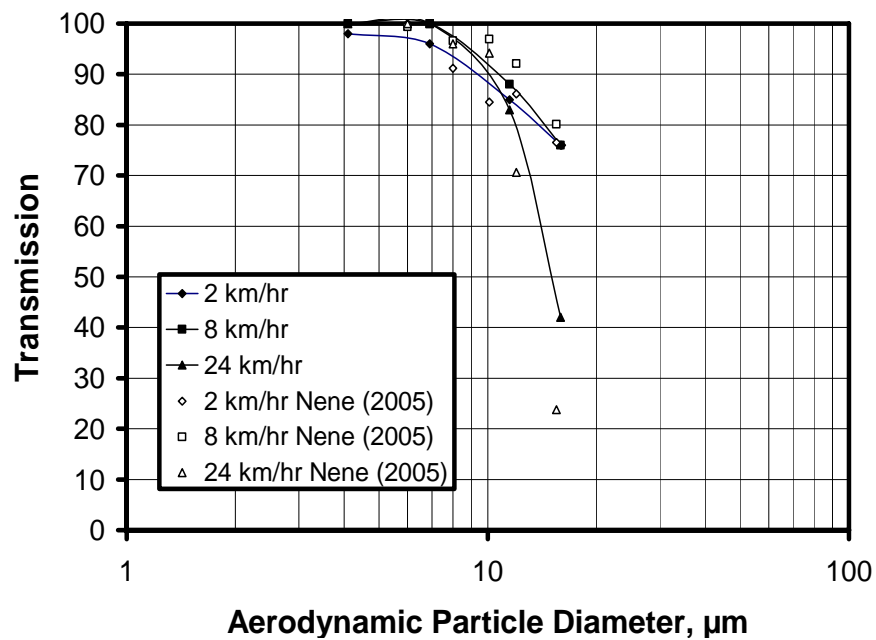**Figure 14:** Photograph of BSI-100 IRI and isokinetic nozzles used in experiments.

Figure 15. Particle diameter vs. transmission for inlet at 100 L/min. No internal fractionator or screen was used in these tests.
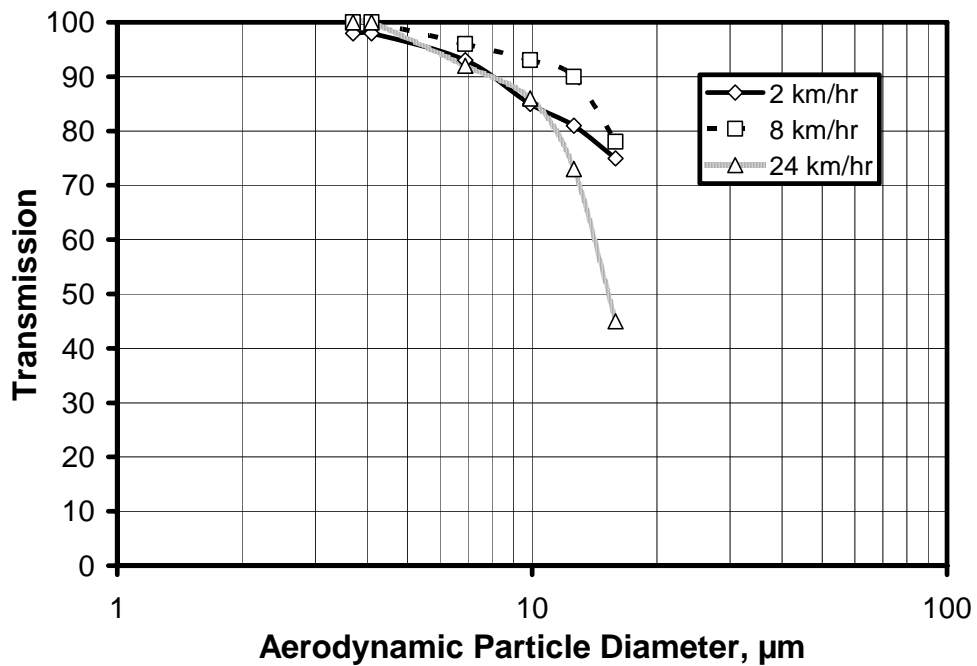
Figure 16. Aerosol transmission through BSI-100 inlet operated at a flow rate of 400 L/min. No internal fractionator or screen.
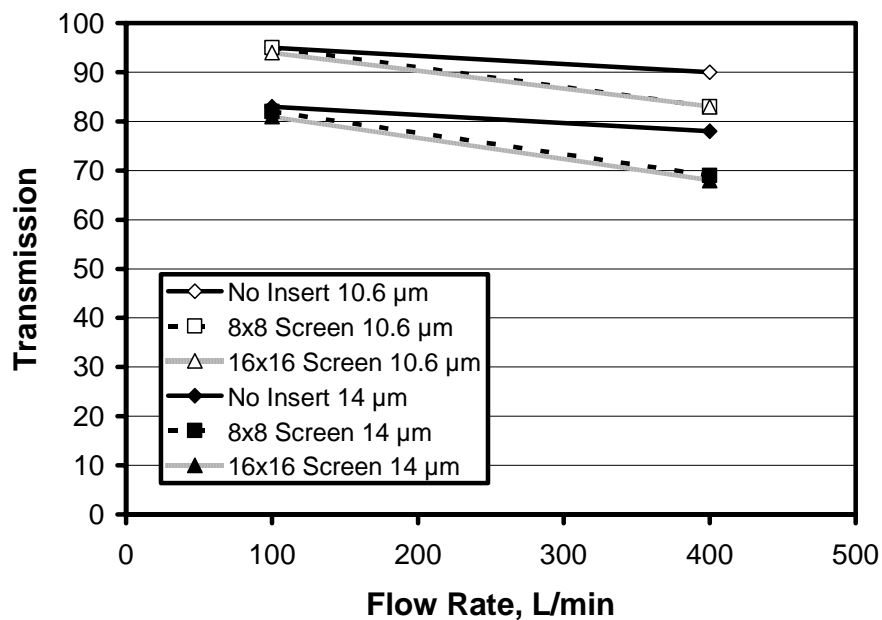
Figure 17. Effect of screens on aerosol transmission through BSI-100 inlet.
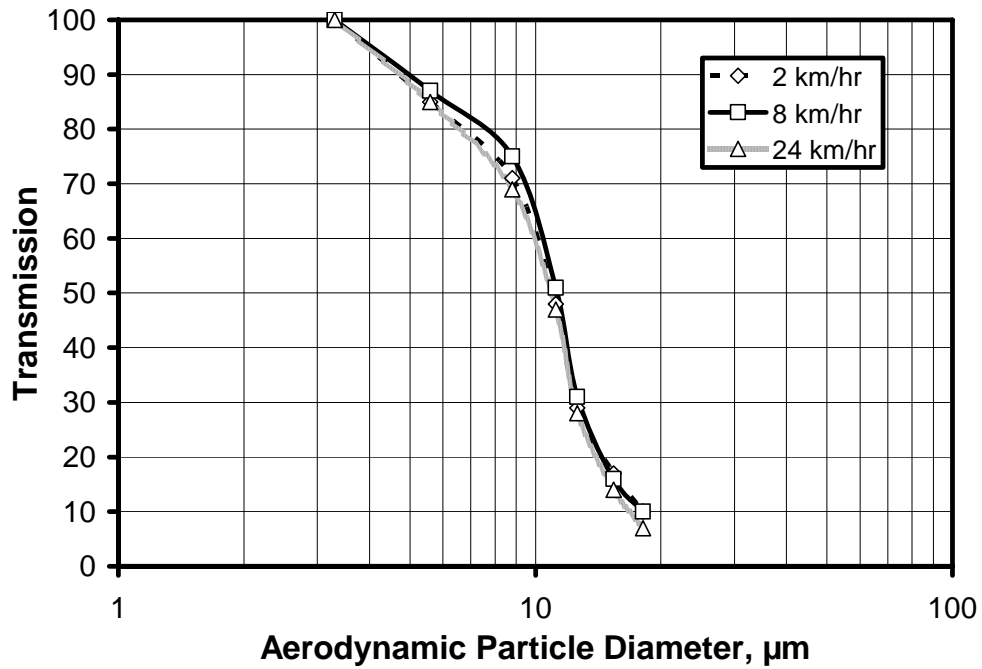
Figure 18: Particle diameter vs. transmission for BSI-100 IRI-100 at 100 L/min.
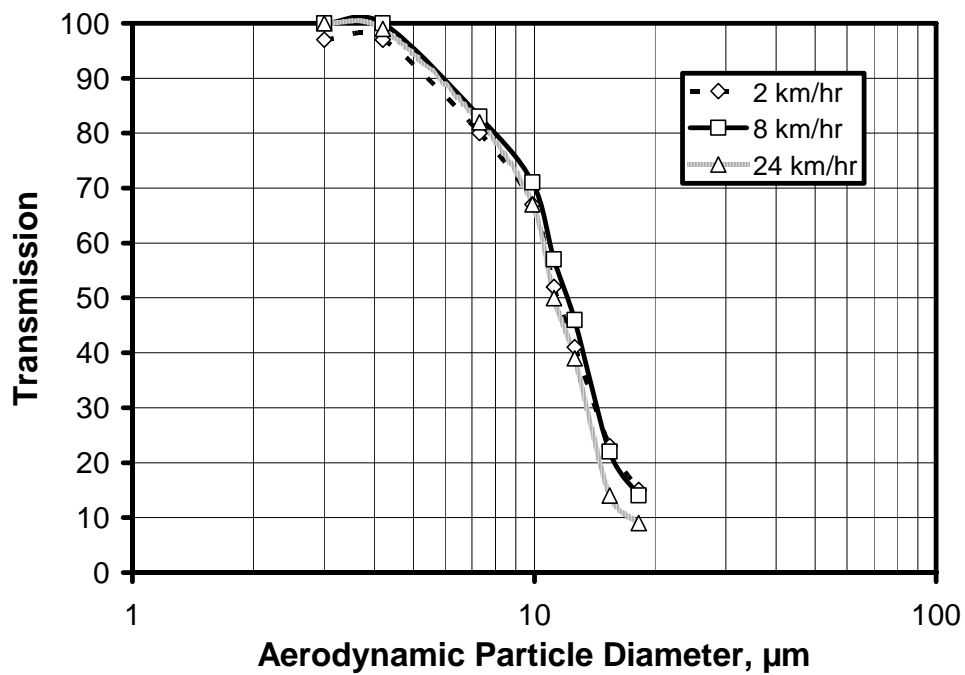
Figure 19. Particle diameter vs. transmission for BSI-100 IRI-400 at 400 L/min.
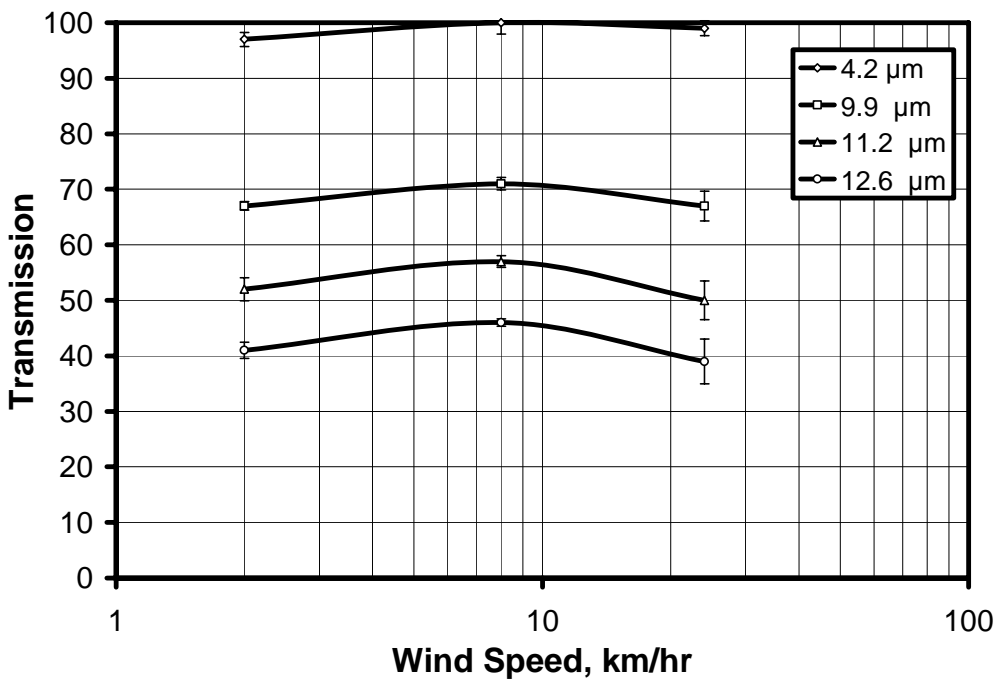
Figure 20. Effect of wind speed on transmission through a BSI-100/IRI-400 at 400 L/min.
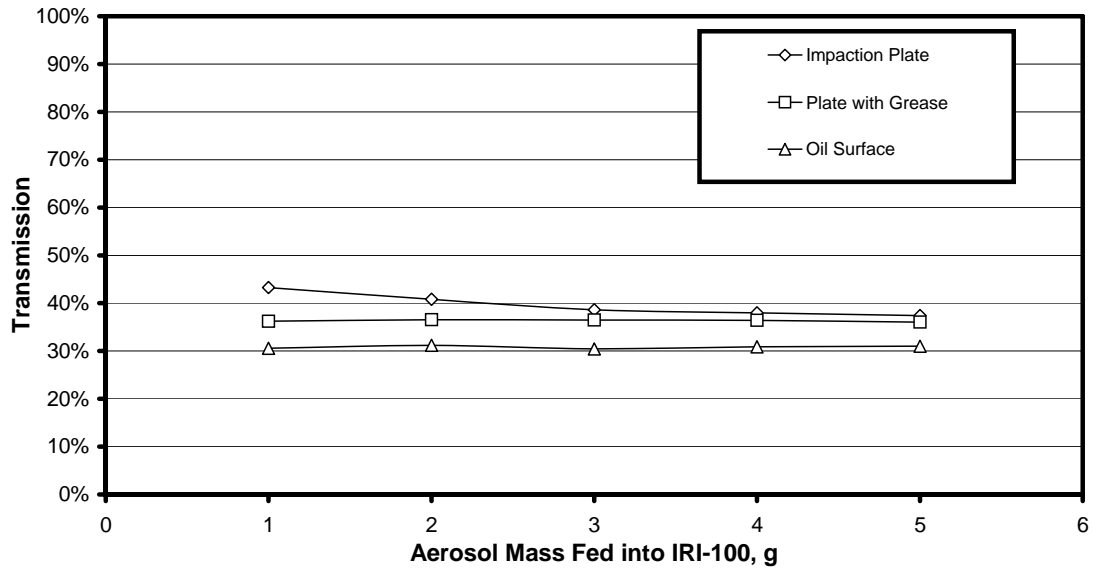
Figure 21: Effect of dust load on transmission of Fine Arizona Road Dust through an IRI-100. No BSI-100 Inlet or screen.
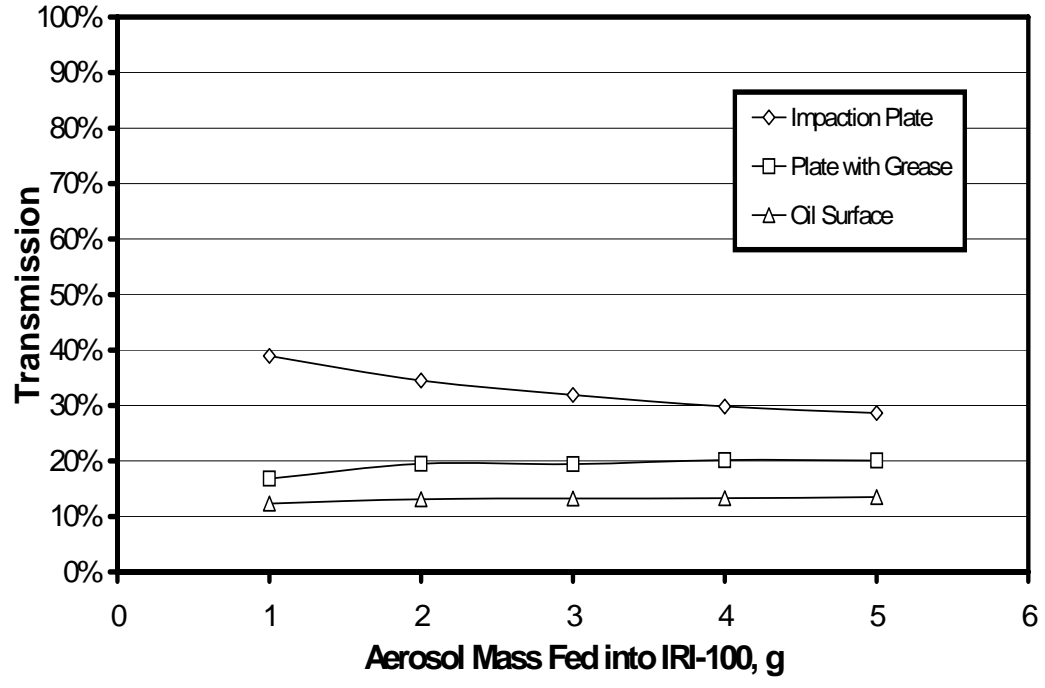
Figure 22: Effect of dust load on transmission of Coarse Arizona Road Dust through an IRI-100. No BSI-100 Inlet or screen.
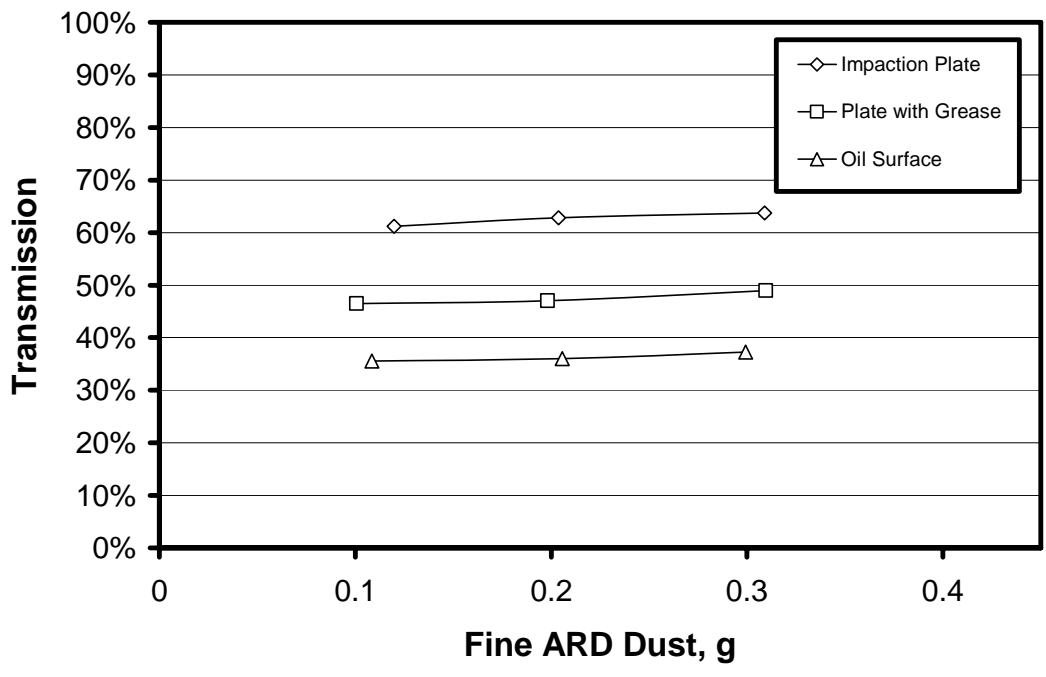
Figure 23: Effect of dust load on transmission of Fine Arizona Road Dust through an IRI-400. No BSI-100 Inlet or screen.
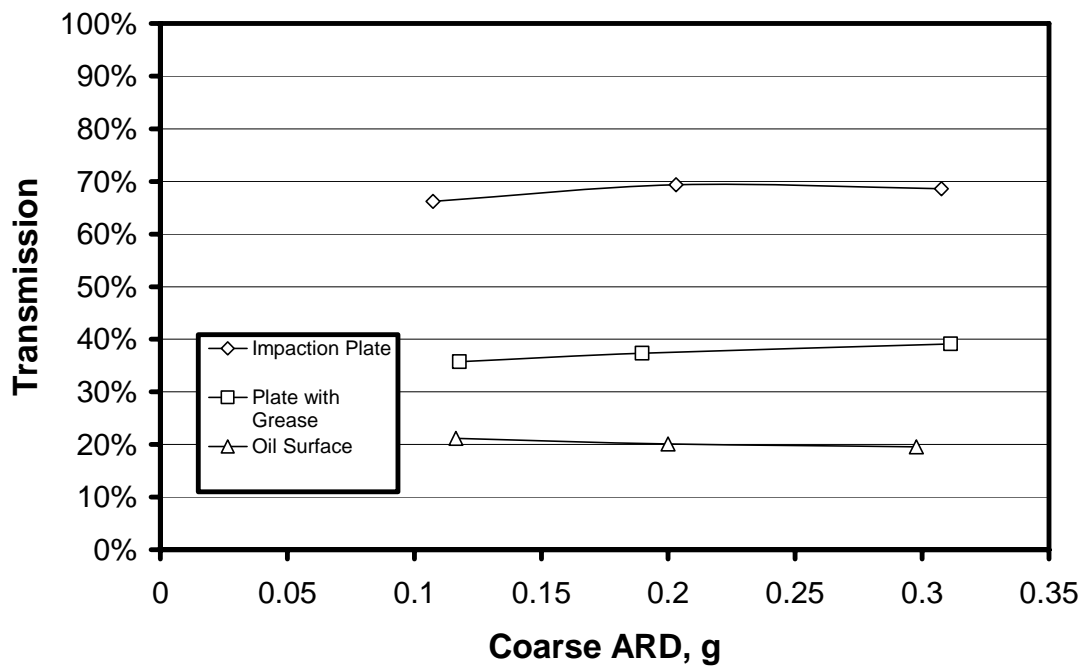
Figure 24: Effect of dust load on transmission of Coarse Arizona Road Dust through an IRI-400. No BSI-100 Inlet or screen.
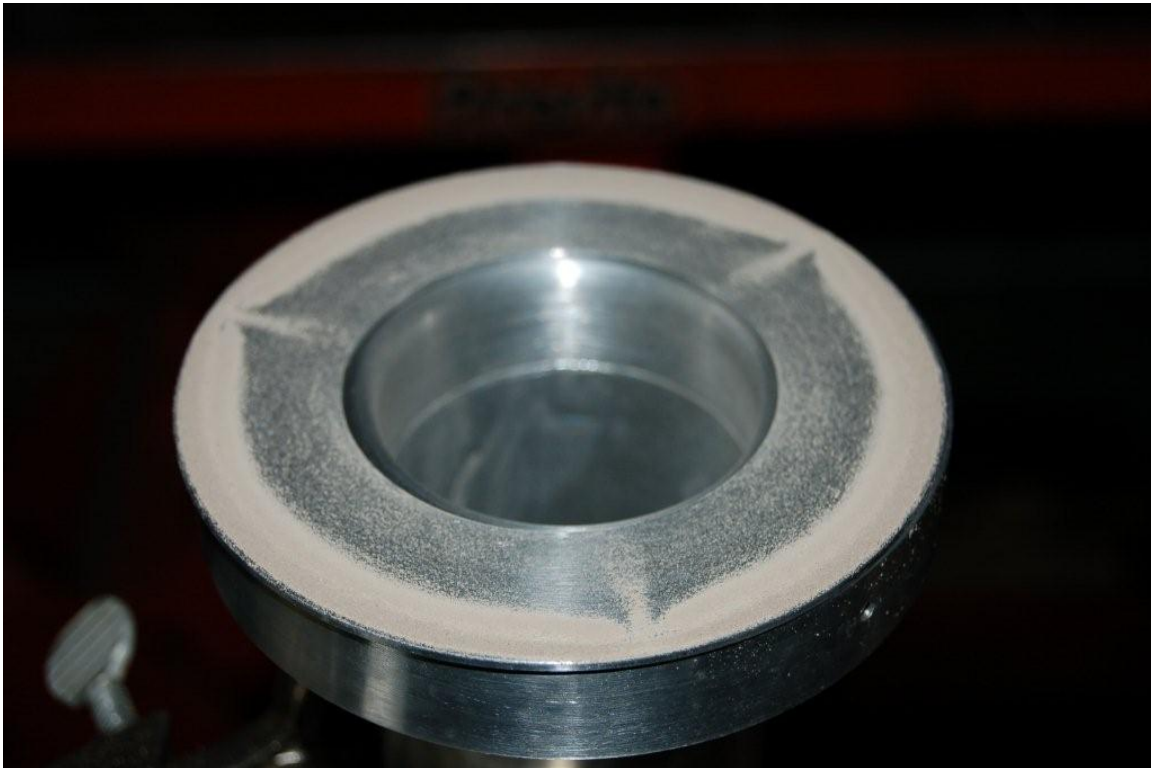
Figure 25: Fine ARD test dust collected on a plain impaction plate in the IRI-100. Most dust is sitting loosely on the impaction plate.

Figure 26: Fine ARD collected on a grease coated impaction plate in an IRI-100. Some dust is wetted by the grease but excess dust is sitting loosely on top of the other particles in the outer region of the collection surface, which is under the impaction jet.

Figure 27: Fine ARD collected on an oil soaked porous media collection surface in an IRI-100. All particles are fully wetted by the oil.
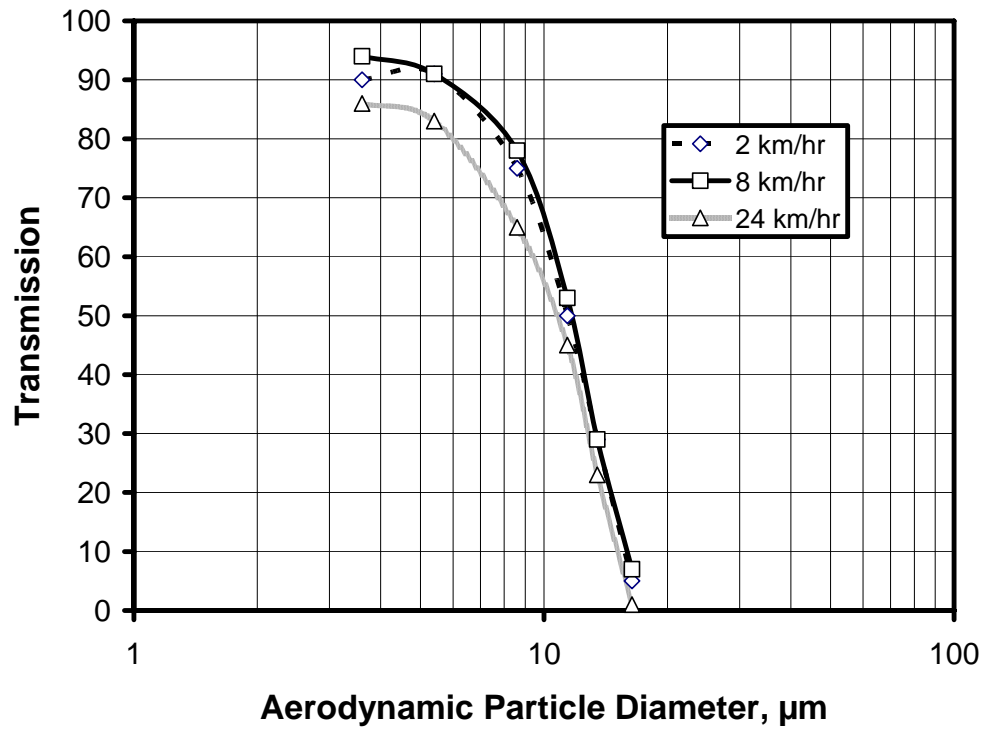
Figure 28: Transmission of aerosol particles through a BSI-100/IVI-100 at 100 L/min.
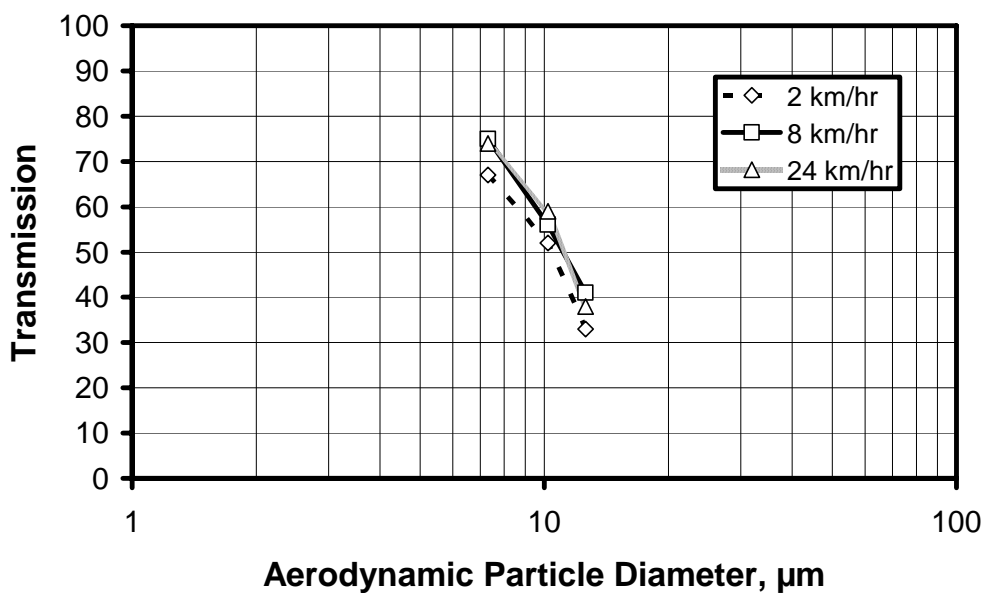
Figure 29: Transmission of aerosol particles through a BSI-100/IVI-300 at 300 L/min.
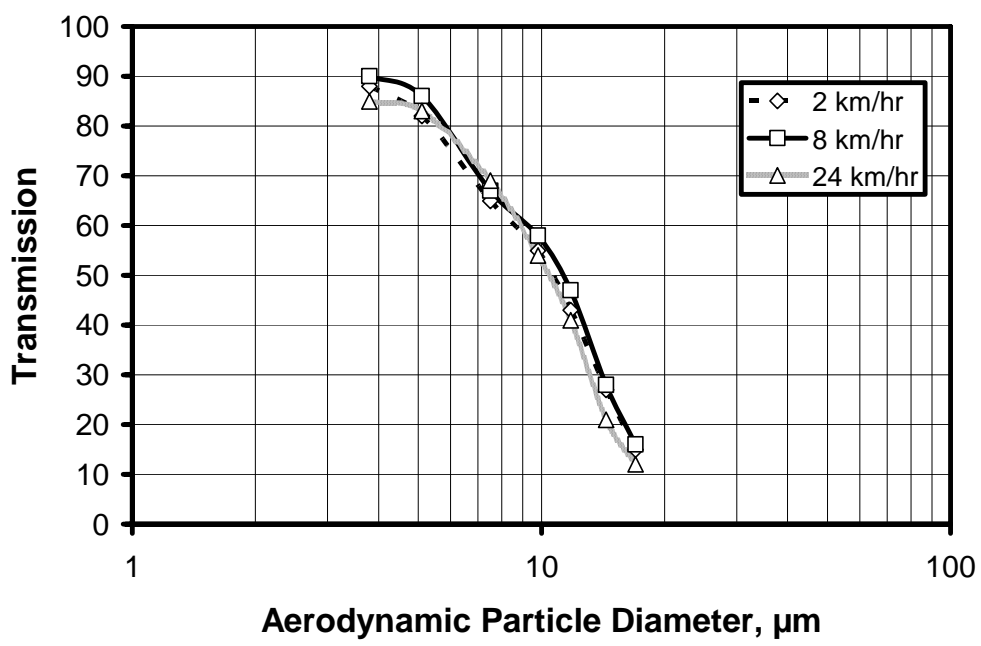
Figure 30: Transmission of aerosol particles through a BSI-100/IVI-400 at 400 L/min.
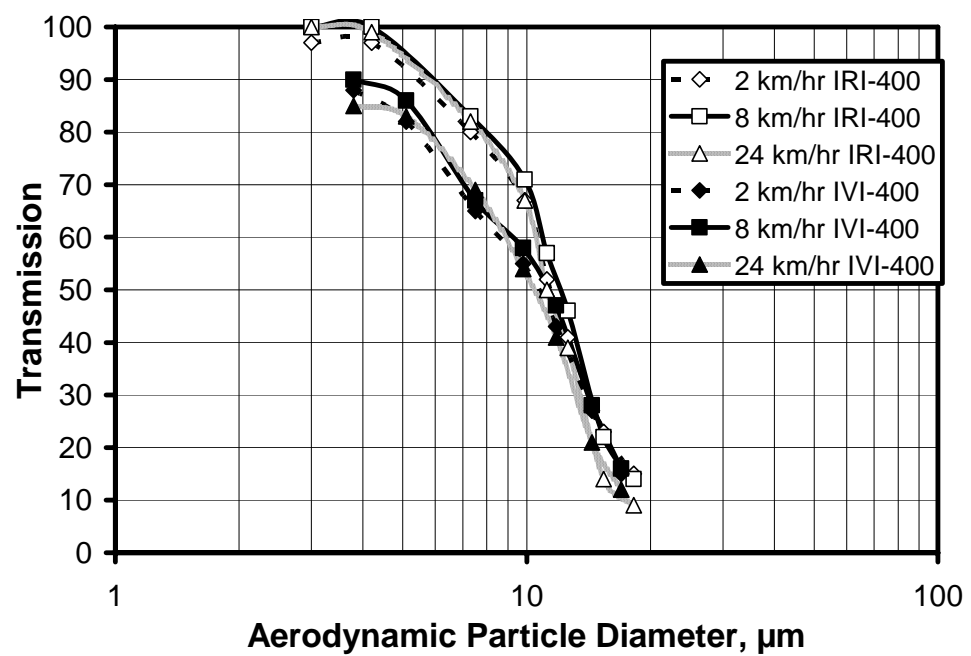
Figure 31: Particle diameter vs. transmission for comparison of IVI-400 vs. IRI-400.

Table 3: Tests of Screens with Different Particle Sizes and Wind Speeds. No Pre-separator.

BSI-100	Tests of Screens with Different Particle Sizes and Wind Speeds. No Pre-separator.				
Apparatus	Flow Rate (L/min)	Wind Speed (km/hr)	Particle Size (μm AD)	Transmission (%)	Standard Deviation
BSI-100	100	8	10.6	95	2.02
8x8	100	8	10.6	95	3.6
16x16	100	8	10.6	94	1.64
BSI-100	400	8	10.6	90	0.87
8x8	400	8	10.6	83	0.85
16x16	400	8	10.6	83	0.72
BSI-100	100	8	14	83	1.75
8x8	100	8	14	82	2.6
16x16	100	8	14	81	2.96
BSI-100	400	8	14	78	0.9
8x8	400	8	14	69	0.84
16x16	400	8	14	68	0.56

Table 4: Test of Aspiration Section at 100 L/min with Different Particle Sizes and Wind Speeds. No Pre-separator.

BSI-100	Test of Aspiration Section at 100 L/min with Different Particle Sizes and Wind Speeds. No Pre-separator.				
Apparatus	Flow Rate (L/min)	Wind Speed (km/hr)	Particle Size (μm AD)	Transmission (%)	Standard Deviation
BSI-100	100	2	4.1	98	0.33
BSI-100	100	8	4.1	100	4.02
BSI-100	100	24	4.1	100	2.85
BSI-100	100	2	6.9	96	4.89
BSI-100	100	8	6.9	100	3.58
BSI-100	100	24	6.9	100	1.56
BSI-100	100	8	10.6	90	3.77
BSI-100	100	2	11.5	85	2.51
BSI-100	100	8	11.5	88	0.12
BSI-100	100	24	11.5	83	1.56
BSI-100	100	8	11.8	83	1.95
BSI-100	100	2	15.9	76	2.28
BSI-100	100	8	15.9	76	0.45
BSI-100	100	24	15.9	42	1.36
BSI-100	100	2	16	76	2.05

Table 5: Test of Aspiration Section at 400 L/min with Different Particle Sizes and Wind Speeds. No Pre-separator.

BSI-100	Test of Aspiration Section at 400 L/min with Different Particle Sizes and Wind Speeds. No Pre-separator.				
Apparatus	Flow Rate (L/min)	Wind Speed (km/hr)	Particle Size (µm AD)	Transmission (%)	Standard Deviation
BSI-100	400	2	3.7	98	0.92
BSI-100	400	8	3.7	100	1.45
BSI-100	400	24	3.7	100	0.51
BSI-100	400	2	4.1	98	1.76
BSI-100	400	8	4.1	100	0.19
BSI-100	400	24	4.1	100	1.47
BSI-100	400	2	6.9	93	3.63
BSI-100	400	8	6.9	96	1.27
BSI-100	400	24	6.9	92	2.63
BSI-100	400	2	9.9	85	3.15
BSI-100	400	8	9.9	93	0.85
BSI-100	400	24	9.9	86	3.25
BSI-100	400	2	12.6	81	2.64
BSI-100	400	8	12.6	90	0.33
BSI-100	400	24	12.6	73	1.92
BSI-100	400	2	15.9	75	2.08
BSI-100	400	8	15.9	78	1.61
BSI-100	400	24	15.9	45	2.91

Table 6: Test of IRI-100 at 100 L/min with Different Particle Sizes and Wind Speeds. With Screen.

BSI-100	Test of IRI-100 at 100 L/min with Different Particle Sizes and Wind Speeds. With Screen.				
Apparatus	Flow Rate (L/min)	Wind Speed (km/hr)	Particle Size (µm AD)	Transmission (%)	Standard Deviation
BSI-100 IRI-100	100	2	3.3	100	2.4
BSI-100 IRI-100	100	8	3.3	100	1.1
BSI-100 IRI-100	100	24	3.3	100	2.8
BSI-100 IRI-100	100	2	5.6	85	0.82
BSI-100 IRI-100	100	8	5.6	87	1.99
BSI-100 IRI-100	100	24	5.6	85	2.07
BSI-100 IRI-100	100	2	8.8	71	0.98
BSI-100 IRI-100	100	8	8.8	75	1.53
BSI-100 IRI-100	100	24	8.8	69	1.23
BSI-100 IRI-100	100	2	11.2	48	1.1
BSI-100 IRI-100	100	8	11.2	51	0.29
BSI-100 IRI-100	100	24	11.2	47	0.4
BSI-100 IRI-100	100	2	12.6	29	1.56
BSI-100 IRI-100	100	8	12.6	31	1.85
BSI-100 IRI-100	100	24	12.6	28	0.71
BSI-100 IRI-100	100	2	15.4	17	0.19
BSI-100 IRI-100	100	8	15.4	16	0.37
BSI-100 IRI-100	100	24	15.4	14	0.62
BSI-100 IRI-100	100	2	18.1	10	0.5
BSI-100 IRI-100	100	8	18.1	10	0.14
BSI-100 IRI-100	100	24	18.1	7	0.72

Table 7: Test of IRI-400 at 400 L/min with Different Particle Sizes and Wind Speeds. With Screen.

BSI-100	Test of IRI-400 at 400 L/min with Different Particle Sizes and Wind Speeds. With Screen.				
Apparatus	Flow Rate (L/min)	Wind Speed (km/hr)	Particle Size (µm AD)	Transmission (%)	Standard Deviation
BSI-100 IRI-400	400	2	3	97	2.33
BSI-100 IRI-400	400	8	3	100	2.42
BSI-100 IRI-400	400	24	3	100	1.07
BSI-100 IRI-400	400	2	4.2	97	1.29
BSI-100 IRI-400	400	8	4.2	100	2.04
BSI-100 IRI-400	400	24	4.2	99	1.34
BSI-100 IRI-400	400	2	7.3	80	1.35
BSI-100 IRI-400	400	8	7.3	83	1.18
BSI-100 IRI-400	400	24	7.3	82	1.51
BSI-100 IRI-400	400	2	9.9	67	0.76
BSI-100 IRI-400	400	8	9.9	71	1.13
BSI-100 IRI-400	400	24	9.9	67	2.68
BSI-100 IRI-400	400	2	11.2	52	2.06
BSI-100 IRI-400	400	8	11.2	57	1.03
BSI-100 IRI-400	400	24	11.2	50	3.51
BSI-100 IRI-400	400	2	12.6	41	1.48
BSI-100 IRI-400	400	8	12.6	46	0.66
BSI-100 IRI-400	400	24	12.6	39	0.6
BSI-100 IRI-400	400	2	15.4	23	1.14
BSI-100 IRI-400	400	8	15.4	22	0.42
BSI-100 IRI-400	400	24	15.4	14	0.26
BSI-100 IRI-400	400	2	18.2	15	0.65
BSI-100 IRI-400	400	8	18.2	14	0.34
BSI-100 IRI-400	400	24	18.2	9	0.97

Table 8: Test of IVI-100 at 100 L/min with Different Particle Sizes and Wind Speeds. With Screen.

BSI-100	Test of IVI-100 at 100 L/min with Different Particle Sizes and Wind Speeds. With Screen.				
Apparatus	Flow Rate (L/min)	Wind Speed (km/hr)	Particle Size (µm AD)	Transmission (%)	Standard Deviation
BSI-100 IVI-100	100	2	3.6	90	0.031
BSI-100 IVI-100	100	8	3.6	94	0.009
BSI-100 IVI-100	100	24	3.6	86	0.05
BSI-100 IVI-100	100	2	5.4	91	0.008
BSI-100 IVI-100	100	8	5.4	91	0.028
BSI-100 IVI-100	100	24	5.4	83	0.023
BSI-100 IVI-100	100	2	8.6	75	0.0198
BSI-100 IVI-100	100	8	8.6	78	0.019
BSI-100 IVI-100	100	24	8.6	65	0.014
BSI-100 IVI-100	100	2	11.4	50	0.02
BSI-100 IVI-100	100	8	11.4	53	0.02
BSI-100 IVI-100	100	24	11.4	45	0.02
BSI-100 IVI-100	100	2	13.5	29	0.013
BSI-100 IVI-100	100	8	13.5	29	0.018
BSI-100 IVI-100	100	24	13.5	23	0.039
BSI-100 IVI-100	100	2	16.4	5	0.02
BSI-100 IVI-100	100	8	16.4	7	0.02
BSI-100 IVI-100	100	24	16.4	1	0.02

Table 9: Test of IVI-300 at 300 L/min with Different Particle Sizes and Wind Speeds. With Screen.

BSI-100	Test of IVI-300 at 300 L/min with Different Particle Sizes and Wind Speeds. With Screen.				
Apparatus	Flow Rate (L/min)	Wind Speed (km/hr)	Particle Size (µm AD)	Transmission (%)	Standard Deviation
BSI-100 IVI-300	300	2	7.3	67	0.6
BSI-100 IVI-300	300	8	7.3	75	1.14
BSI-100 IVI-300	300	24	7.3	74	0.42
BSI-100 IVI-300	300	2	10.2	52	0.26
BSI-100 IVI-300	300	8	10.2	56	0.65
BSI-100 IVI-300	300	24	10.2	59	0.34
BSI-100 IVI-300	300	2	12.6	33	0.97
BSI-100 IVI-300	300	8	12.6	41	1.2
BSI-100 IVI-300	300	24	12.6	38	1.56

Table 10: **Test of IVI-400 at 400 L/min with Different Particle Sizes and Wind Speeds. With Screen.**

BSI-100	Test of IVI-400 at 400 L/min with Different Particle Sizes and Wind Speeds. With Screen.				
Apparatus	Flow Rate (L/min)	Wind Speed (km/hr)	Particle Size (μm AD)	Transmission (%)	Standard Deviation
BSI-100 IVI-400	400	2	3.8	88	2.33
BSI-100 IVI-400	400	8	3.8	90	2.42
BSI-100 IVI-400	400	24	3.8	85	1.07
BSI-100 IVI-400	400	2	5.1	82	1.29
BSI-100 IVI-400	400	8	5.1	86	2.04
BSI-100 IVI-400	400	24	5.1	83	1.34
BSI-100 IVI-400	400	2	7.5	65	1.35
BSI-100 IVI-400	400	8	7.5	67	1.18
BSI-100 IVI-400	400	24	7.5	69	1.51
BSI-100 IVI-400	400	2	9.8	55	0.76
BSI-100 IVI-400	400	8	9.8	58	1.13
BSI-100 IVI-400	400	24	9.8	54	2.68
BSI-100 IVI-400	400	2	11.8	43	2.06
BSI-100 IVI-400	400	8	11.8	47	1.03
BSI-100 IVI-400	400	24	11.8	41	3.51
BSI-100 IVI-400	400	2	14.4	27	1.48
BSI-100 IVI-400	400	8	14.4	28	0.66
BSI-100 IVI-400	400	24	14.4	21	0.6
BSI-100 IVI-400	400	2	17	15	1.14
BSI-100 IVI-400	400	8	17	16	0.42
BSI-100 IVI-400	400	24	17	12	0.26

VITA

Name: Michael Matthew Baehl

Address: MS 3123, Department of Mechanical Engineering, Texas A&M
                   University, College Station, TX 77843

Permanent Address: 1230 Olesen Dr., Naperville, IL., 60540.

Email Address: mbaehl@tamu.edu

Education: B.S., Mechanical Engineering, University of Illinois, Urbana-Champaign,
             2005

             M.S., Mechanical Engineering, Texas A&M University, 2007